

# The Tarantula Nebula as a template for extragalactic star forming regions from VLT/MUSE and HST/STIS

Paul A. Crowther<sup>1</sup>, Saida M. Caballero-Nieves<sup>1,2</sup>, Norberto Castro<sup>3</sup>  
and Christopher J. Evans<sup>4</sup>

<sup>1</sup>Department of Physics & Astronomy, University of Sheffield, Hounsfield Road,  
Sheffield, S3 7RH, UK

email: Paul.Crowther@sheffield.ac.uk

<sup>2</sup>Physics & Space Sciences, Florida Institute of Technology, 150 W. University Blvd,  
Melbourne, FL 32901, USA

<sup>3</sup>Department of Astronomy, University of Michigan, 1805 S.University,  
Ann Arbor, MI 48109, USA

<sup>4</sup>UK Astronomy Technology Centre, Royal Observatory Edinburgh, Blackford Hill,  
Edinburgh, EH9 3HJ, UK

**Abstract.** We present VLT/MUSE observations of NGC 2070, the dominant ionizing nebula of 30 Doradus in the LMC, plus HST/STIS spectroscopy of its central star cluster R136. Integral Field Spectroscopy (MUSE) and pseudo IFS (STIS) together provides a complete census of all massive stars within the central  $30 \times 30$  parsec $^2$  of the Tarantula. We discuss the integrated far-UV spectrum of R136, of particular interest for UV studies of young extragalactic star clusters. Strong He II  $\lambda 1640$  emission at very early ages (1–2 Myr) from very massive stars cannot be reproduced by current population synthesis models, even those incorporating binary evolution and very massive stars. A nebular analysis of the integrated MUSE dataset implies an age of  $\sim 4.5$  Myr for NGC 2070. Wolf-Rayet features provide alternative age diagnostics, with the primary contribution to the integrated Wolf-Rayet bumps arising from R140 rather than the more numerous H-rich WN stars in R136. Caution should be used when interpreting spatially extended observations of extragalactic star-forming regions.

**Keywords.** stars: early-type – stars: Wolf-Rayet – open clusters and associations: individual: NGC 2070 – galaxies: star clusters: individual: R136 – ISM: HII regions

## 1. Introduction to the Tarantula Nebula

Our interpretation of distant, unresolved star-forming regions relies heavily upon population synthesis models, including Starburst99 (Leitherer *et al.* 2014) and BPASS (Eldridge & Stanway 2012). However, such models rely on a number of key assumptions, involving the initial mass function (IMF), rotation, star formation history. In particular, the post-main sequence evolution of massive stars depends sensitively on internal mixing processes and adopted mass-loss prescriptions. Locally, close binary evolution looks to play a major role (Sana *et al.* 2012) and there is some evidence that the upper IMF extends well beyond the usual  $M_{\max} \sim 100M_{\odot}$  (Crowther *et al.* 2010).

Therefore, it is important to benchmark population synthesis models against empirical results from nearby, resolved star-forming regions. Within the Local Group of galaxies, the LMC’s Tarantula Nebula is the closest analogue to the intensive star-forming clumps of high-redshift galaxies (Jones *et al.* 2010). Kennicutt (1984) compares the nebular properties of nearby extragalactic HII regions, including the Tarantula (alias 30 Doradus). Although the Tarantula Nebula extends over several hundred parsecs, the central ionizing

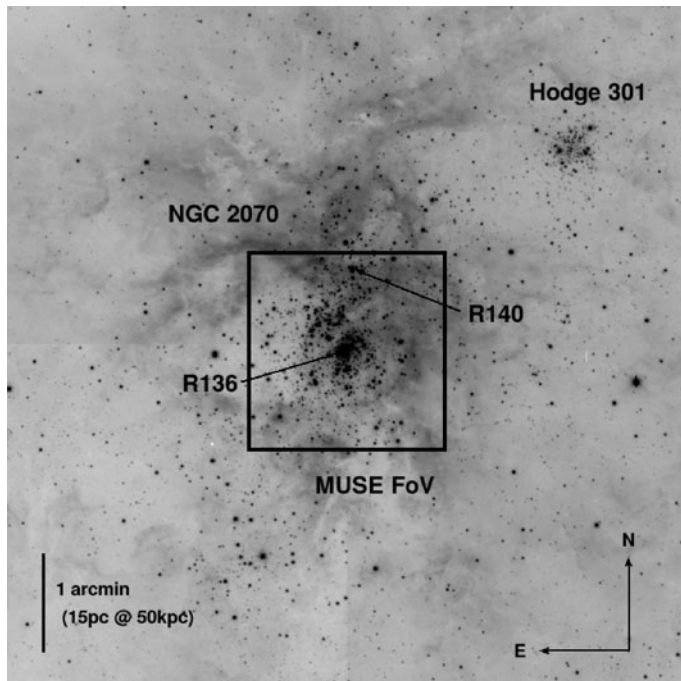


**Figure 1.** VLT/FORS2 R-band image of the central  $6 \times 6$  arcmin $^2$  of the Tarantula Nebula, corresponding to  $100 \times 100$  parsec at the 50 kpc LMC distance, indicating NGC 2070, R136, R140, Hodge 301 and the VLT/MUSE field of view.

region, NGC 2070, spans 40 pc, with the massive, dense cluster R136† at its core (see Table 1 of Walborn 1991).

In this work, we exploit the high spatial resolution of HST to dissect the central  $4 \times 4$  arcsec $^2$  of the R136 star cluster (Crowther *et al.* 2016) plus the new VLT large field-of-view integral field spectrograph MUSE which has observed the central  $2 \times 2$  arcmin $^2$  region of NGC 2070 (N. Castro *et al.* in prep.). Figure 1 shows a VLT/FORS2 R-band image of the central region of the Tarantula, including NGC 2070 and an older star cluster (Hodge 301)  $3'$  to the NW. Comparisons with population synthesis predictions are made to assess their validity for young starburst regions.

## 2. HST/STIS ultraviolet spectroscopy of R136

R136 is the young massive star cluster at the core of the Tarantula Nebula. Establishing the stellar content of R136 has generally required high spatial spectroscopy from HST at UV and optical wavelengths or a ground-based 8m telescope with Adaptive Optics. Massey & Hunter (1998) have used HST/FOS to observe stars in the R136 region (few parsec), while Crowther *et al.* (2016) used HST/STIS to map the core of R136, obtaining complete UV/optical spectroscopy of the central parsec. Spectroscopic analysis of the brightest 52 O stars reveals a cluster age of  $1.5^{+0.3}_{-0.7}$  Myr, confirming this as one of the youngest massive clusters in the Local Group.

The integrated UV spectrum of R136 exhibits strong stellar C IV  $\lambda\lambda 1548-51$ , N V  $\lambda\lambda 1238-42$  P Cygni profiles plus prominent He II  $\lambda 1640$  emission. Within unresolved high

† Strictly, the star cluster is R136a, with R136b and R136c representing individual very massive stars, but R136 is generally used to describe the cluster

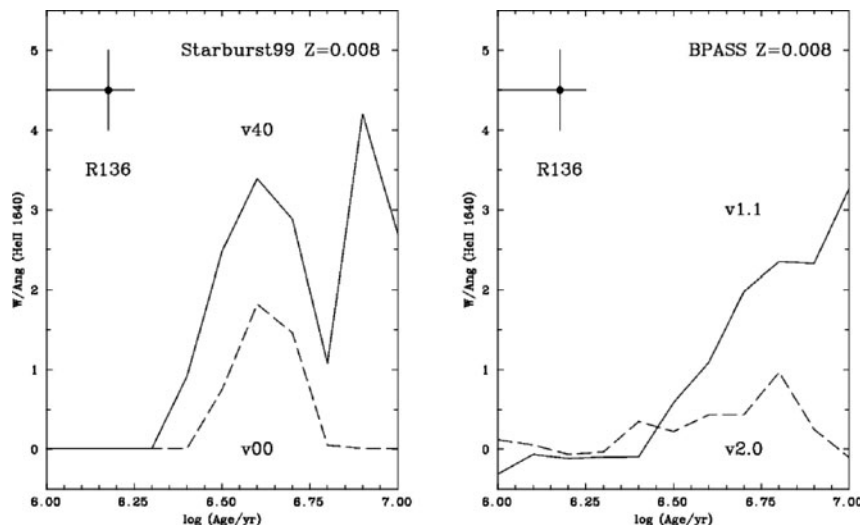


**Figure 2.** Comparison between observed He II  $\lambda 1640$  emission in R136 (Crowther *et al.* 2016) and  $Z = 0.008$  instantaneous burst models from (left): Starburst99 (Leitherer *et al.* 2014) for non-rotating (v00, dashed) and rotating (v40, solid) Geneva single star models with  $M_{\max} = 120M_{\odot}$ , (right): BPASS (Eldridge & Stanway 2012, Stanway *et al.* 2016) close binary models for  $M_{\max} = 100M_{\odot}$  (v1.1, solid) and  $M_{\max} = 300M_{\odot}$  (v2.0, dashed).

mass star clusters, He II  $\lambda 1640$  emission is usually believed to originate from classical He-burning Wolf-Rayet (WR) stars which become prominent after several Myr. The presence of strong He II emission in the young R136 indicates a different origin, namely the presence of very massive stars (VMS,  $M_{\text{init}} \geq 100M_{\odot}$ ). Indeed,  $\sim 10$  VMS within the central parsec contribute one third of the integrated far-UV continuum, and dominate the observed He II emission.

Standard population synthesis models fix the upper mass limit at  $M_{\max} \sim 100M_{\odot}$ , so fail to produce significant He II  $\lambda 1640$  emission until  $\sim 2$ – $3$  Myr after the initial burst, as illustrated in the left panel of Fig 2, which compares predictions from Starburst99 based on metal-poor ( $Z = 0.008$ ) Geneva models (Leitherer *et al.* 2014) with the observed strong, broad He II emission in R136 (Crowther *et al.* 2016). These predictions are based on single, non-rotating (v00) or rotating (v40) models, so exclude the contribution of close binary evolution and VMS. Close binary evolution has been included into metal-poor  $Z = 0.008$  BPASS burst models (v1.1, Eldridge & Stanway 2012), which is presented on the right panel of Fig. 2 together with recent updates (v2.0, Stanway *et al.* 2016) in which very massive stars are incorporated. Weaker emission in the more recent models for ages of  $\geq 3$  Myr results from the use of different spectral libraries.

It is apparent that both single and binary population synthesis models currently fail to reproduce the observed strong He II  $\lambda 1640$  in R136, indicating an incomplete treatment of rotation, binarity and mass-loss for the most massive stars in star clusters. In the nearby universe, a number of young massive star clusters also exhibit strong He II  $\lambda 1640$  emission (Wofford *et al.* 2014, Smith *et al.* 2016) while it is a prominent (stellar and nebular) spectral feature in the integrated rest-frame UV light of high redshift Lyman Break galaxies (Shapley *et al.* 2003). VMS and classical WR stars will initially play a major role in stellar He II  $\lambda 1640$  emission, with close binary evolution subsequently dominant.

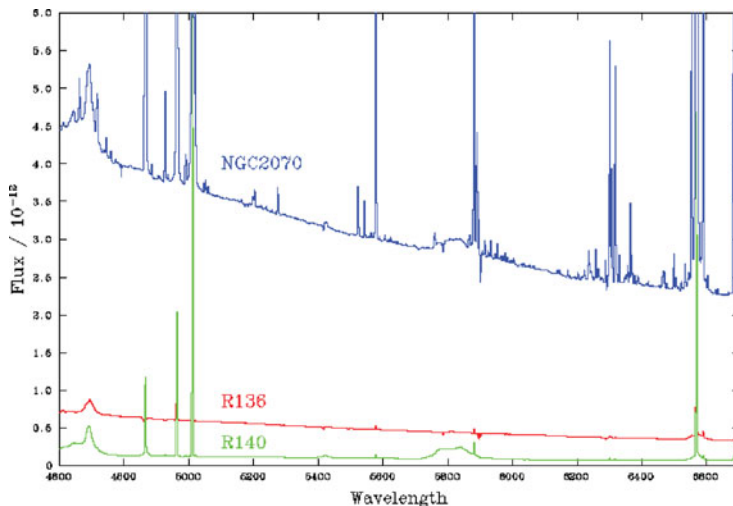


**Figure 3.** Integrated VLT/MUSE spectrum of NGC 2070 from N. Castro *et al.* (in prep), highlighting strong blue ( $\text{He II } \lambda\lambda 4686, \text{C III } \lambda\lambda 4647-51$ ) and yellow ( $\text{C IV } \lambda\lambda 5801-12$ ) Wolf-Rayet features, including the individual contributions from R136 and R140.

### 3. VLT/MUSE integral field spectroscopy of NGC 2070

Individual massive stars within NGC 2070 – the dominant HII region within the Tarantula Nebula – have been extensively investigated from the ground (Melnick 1985, Walborn & Blades 1997, Bosch *et al.* 1999, Evans *et al.* 2011), but the advent of large field-of-view integral field spectrographs such as MUSE permit the integrated properties of nearby giant HII regions to be investigated. We have obtained four pointings of VLT/MUSE which cover the central region of NGC 2070 (Fig. 1), and provide medium resolution optical spectroscopic observations ( $R = 3,000$ ,  $\lambda = 4600-9360\text{\AA}$ ) of the  $2\times 2$  arcmin $^2$  region, sampled at 0.3 arcsec spaxel $^{-1}$ .

Nebular and stellar kinematics of NGC 2070 are discussed in N. Castro *et al.* (in prep), while the individual stellar content will be discussed elsewhere. Here we focus upon the integrated stellar and nebular properties of the VLT/MUSE dataset, which samples a  $30\times 30$  parsec $^2$  region of NGC 2070, including R136. At a distance of 10 Mpc, this region would subtend only 0.6 arcsec, typical of long-slit spectroscopy of extragalactic HII regions from large ground-based telescopes. The integrated VLT/MUSE spectrum of NGC 2070 is presented in Fig. 3, revealing prominent nebular emission features. An interstellar extinction of  $E(B-V) = 0.38$  follows from the observed  $\text{H}\alpha/\text{H}\beta$  flux ratio, in good agreement with Pellegrini *et al.* (2010), while the measured  $\text{H}\alpha$  flux is 60% of that measured by Kennicutt *et al.* (1995) for a 3' radius centred upon R136, such that the inferred  $\text{H}\alpha$  luminosity,  $\log L(\text{H}\alpha) = 39.1$  erg s $^{-1}$ , corresponds to 10% of the total emission from the Tarantula Nebula (Kennicutt 1984).

Commonly used diagnostics to estimate the age of young extragalactic star forming regions are nebular Balmer emission and the presence of WR features in the integrated light. We infer an age of  $\sim 4.5$  Myr from  $\log W_\lambda(\text{H}\alpha)/\text{\AA} = 2.85$  for NGC 2070, even though it is clear that the individual ages of massive stars within NGC 2070 span a broad range (e.g. Selman *et al.* 1999, F. Schneider *et al.* in prep) with massive star formation still ongoing in NGC 2070 (Walborn *et al.* 2013) plus Hodge 301 to the NW of NGC 2070 indicating a burst of star formation 15–25 Myr ago. Recalling Fig. 3, both the blue ( $\text{He II } \lambda\lambda 4686, \text{C III } \lambda\lambda 4647-51$ ) and yellow ( $\text{C IV } \lambda\lambda 5801-12$ ) WR features are prominent in the integrated VLT/MUSE dataset, with  $W_\lambda(\text{blue}) \sim 12\text{\AA}$ , and  $W_\lambda(\text{yellow}) \sim 9\text{\AA}$ . As with

He II  $\lambda 1640$  in ultraviolet spectroscopy, it is usually assumed that WR bumps arise from classical He-burning stars. Indeed, for a burst age of 4–5 Myr, Starburst99 models at  $Z = 0.008$  predict  $W_\lambda(\text{blue}) \sim 15\text{\AA}$  (5\text{\AA}) and  $W_\lambda(\text{yellow}) \sim 6\text{\AA}$  (3\text{\AA}) from v40 rotating (v00 non-rotating) models.

Therefore, at face value it appears that a single 4–5 Myr burst is reasonably consistent with the observed nebular and stellar line features in NGC 2070. However, integral field spectroscopy also permits us to consider the origin of these WR features within NGC 2070. Fig. 3 also displays the integrated spectrum of R136, which exhibits weak He II  $\lambda 4686$  emission from the VMS in this young  $\sim 1.5$  Myr cluster, contributing only 15% of the blue NGC 2070 WR feature, and crucially negligible emission at C IV  $\lambda\lambda 5801-12$  since it is too young to host any WC stars. Indeed, the dominant source of the yellow WR feature in NGC 2070 is R140, a relatively modest group of stars including two classical WN stars and a WC star (indicated in Fig. 1, while R140 also contributes 25% of the integrated blue WR feature. The higher line luminosities of classical WR stars (in R140) with respect to H-rich WN stars (in R136) compensate for their reduced population.

Therefore caution should be used when interpreting spatially extended regions in extragalactic star forming regions. In the absence of spatially resolved spectroscopy, one would anticipate that the integrated stellar and nebular properties of NGC 2070 are dominated by the R136 region, whereas the nebular-derived age represents a composite of the young R136 cluster and older OB stars, while the stellar-derived age is biased towards WR stars possessing the highest line luminosities (R140), rather than those within the dominant ionizing cluster (R136). By way of example, the dominant cluster in NGC 3125-A has an age of 1–2 Myr (Wofford *et al.* 2014) while a burst age of 4 Myr is inferred from its associated star-forming region from nebular and WR diagnostics (Hadfield & Crowther 2006).

## References

- Bosch, G., Terlevich, R., Melnick, J., & Selman, F. 1999, *A&AS* 137, 21  
 Crowther, P. A., Schnurr, O., Hirschi, R. *et al.* 2010, *MNRAS* 408, 731  
 Crowther, P. A., Caballero-Nieves, S., Boestrom, K. A. *et al.* 2016, *MNRAS* 458, 624  
 Eldridge, J. J. & Stanway, E. R. 2012, *MNRAS* 419, 479  
 Evans, C. J., Taylor, W. D., Henault-Brunet, V. *et al.* 2011, *A&A* 530, A108  
 Hadfield, L. J. & Crowther, P. A. 2006, *MNRAS* 368, 1822  
 Kennicutt, R. C. Jr 1984, *ApJ* 287, 116  
 Kennicutt, R. C. Jr, Bresolin, F., Bomans, D. J., Bothun, G. D., & Thompson, I. B. 1995, *AJ* 109, 594  
 Jones, T. A., Swinbank, A. M., Ellis, R. S., & Stark, D. P. 2010, *MNRAS* 404, 1247  
 Massey, P. & Hunter, D. A. 1998, *ApJ* 493, 180  
 Melnick, J. 1985, *A&A* 153, 235  
 Pellegrini, E. W., Baldwin, J. A., & Ferland, G. J. 2010, *ApJS* 191, 160  
 Sana, H., de Mink, S. E., de Koter, A. *et al.* 2012, *Science* 337, 444  
 Selman, F., Melnick, F., Bosch, G., & Terlevich, R. 1999, *A&A* 347, 532  
 Shapley, A. E., Steidel, C. C., Pettini, M., & Adelberger, K. L. 2003, *ApJ* 588, 65  
 Smith, L. J., Crowther, P. A., Calzetti, D., & Sidoli, F. 2016, *ApJ* 823, 38  
 Stanway, E. R., Eldridge, J. J. & Becker G. D. 2016, *MNRAS* 456, 485  
 Walborn, N. R. 1991, in: Haynes, R. & Milne, D. (eds.), *The Magellanic Clouds*, Proceedings of IAU Symposium No. 148, (Dordrecht: Kluwer), p. 145  
 Walborn, N. R. & Blades, C. J. 1997, *ApJS* 112, 457  
 Walborn, N. R., Barba, R. H., & Sewilo, M. M. 2013, *AJ* 145, 98  
 Wofford, A., Leitherer, C., Chandar, R., & Bouret, J.-C. 2014, *ApJ* 781, 122